# Accepted Manuscript

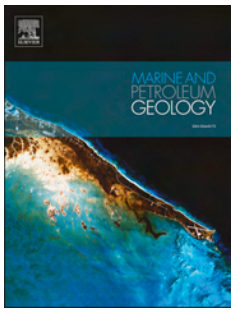


Seepage rate of hydrothermally generated petroleum in East African Rift lakes: An example from Lake Tanganyika

Davide Oppo, Andrew Hurst

PII: S0264-8172(18)30077-1

DOI: 10.1016/j.marpetgeo.2018.02.031

Reference: JMPG 3259

To appear in: *Marine and Petroleum Geology*

Received Date: 1 December 2017

Revised Date: 19 February 2018

Accepted Date: 20 February 2018

Please cite this article as: Oppo, D., Hurst, A., Seepage rate of hydrothermally generated petroleum in East African Rift lakes: An example from Lake Tanganyika, *Marine and Petroleum Geology* (2018), doi: 10.1016/j.marpetgeo.2018.02.031.

**Highlights**

- The average annual total seepage rate in the Cape Kalumba seeps is 138.7 $m^3$
- Oil emission from single seeps is consistent with globally-significant provinces
- Oil migrates along strata toward lake border faults and seeps in the water column
- Rapid generation of unconventional hydrothermal petroleum may occur in rift lakes
- The petroleum system generating the oil seeps lacks of accumulation capabilities

# Seepage rate of hydrothermally generated petroleum in East African Rift lakes: an example from Lake Tanganyika

Davide Oppo[1*] & Andrew Hurst[1]

[1] *School of Geosciences, University of Aberdeen, King's College, Aberdeen AB24 3UE, UK*
**Correspondence: davide.oppo@abdn.ac.uk*

Keywords: Hydrothermal petroleum; Rift Lake; Lake Tanganyika; Oil seep; East African Rift; Synthetic Aperture Radar

**Abstract**

Synthetic Aperture Radar images provide temporal coverage of the oil seepage recurrence at Cape Kalumba, Lake Tanganyika. In combination with legacy seismic data, it has been possible to reconstruct the geological context that regulates seepage and estimate the oil seepage rates. Oil seepage is along fractures associated with the East Ubwari Faults, which in turn promote an active hydrothermal system that matures very shallow (10's m below the lake floor) oil-prone, less than 25 kyr old source rocks. Temporally consistent oil slick origin points are preferentially aligned E-W and SE-NW, and feed oil slicks on the lake surface. Pervasive seeps activity with significant emission rates, up to 449.39 $m^3y^{-1}$, proves the presence of high-quality oil-prone source rocks and an active petroleum system that emits oil to form slicks. Hydrothermally-driven source rock maturation occurring at very shallow depth creates a narrow depth-window for conventional trapping of oil. Elsewhere in the lakes of the East African Rift, where similar hydrothermal systems occur, oil slicks may only be indicative of active petroleum systems without the presence of conventional traps.

## 1. Introduction

The spontaneous leakage of oil and gas is recorded as oil slicks on the surface of water bodies, is a prime indication of an active petroleum system in the host basin (Aminzadeh et al., 2013; Orange et al., 2009). Since the beginning of modern petroleum exploitation, cold seepage has been regularly used to support efficacious exploration and to recover information on the associated hydrocarbons occurring in deep reservoirs (e.g. Vis, 2017). Remote-sensing is increasingly used to identify spontaneous petroleum seepage on land and offshore (MacDonald et al., 2015), and to differentiate and track anthropogenic - oil spills (Hu et al., 2011; MacDonald et al., 2015). Satellite Synthetic Aperture Radar (SAR) images have demonstrated their efficiency in detecting offshore natural hydrocarbon seepage (Espedal and Twahl, 1999; Garcia-Pineda et al., 2010; Wang et al., 2013) and in supporting the quantification and description of frequency and rates of oil leakage at both regional and local scales (Jatiault et al., 2017; Körber et al., 2014; MacDonald et al., 1996; Vis, 2017).

Spontaneous oil seepage drove the initial phases of petroleum exploration in East Africa at the beginning of the 20$^{th}$ century and rift lakes are recognized for petroleum prospectivity (Roberts et al., 2015; Scholz and Rosendahl, 1990; Talbot, 1988). A prime example is the Albertine Graben, where diffused oil seeps and slicks are the surficial manifestation of the significant oil reserves hosted in the subsurface of Lake Albert (Van Dort et al., 2010). Lake Tanganyika is one of the major East African Rift lakes. Despite the absence of commercially-significant oil discoveries within its basin so far, it hosts significant oil seeps in comparison with other East African lakes: the Cape Kalumba seeps (e.g. Simoneit et al., 2000). These seeps are located 3-4 km offshore of Cape Kalumba in the southern Ubwari Peninsula (Fig. 1). The seeps were first described at the end of 19$^{th}$ century by Nicolas (1898) who documented the expulsion of asphalt and bursting steam jets in the open water of the lake. More recent observations documented active bubbling of gaseous and liquid hydrocarbons on the lake

surface (Simoneit et al., 2000). The seeping oil forms slicks on the lake and is transported along the coast by surface currents, commonly accumulating as tar balls on the coastline of Ubwari Peninsula (J. Tiercelin et al., 1993).

The oil geochemistry of Cape Kalumba seeps has been described in various scientific publications. However, the rates of oil emission and the subsurface setting associated with hydrocarbon origin and migration have never been investigated. This work analyses multi-temporal SAR scenes acquired in the area offshore Cape Kalumba to document and describe the spatiotemporal evolution of the slicks and the related emission points. Interpretation of legacy seismic data (Rosendahl, 1988) allows the correlation of seeps expression on lake surface with their possible emission points on the lake bed, and the recognition of the structural and/or stratigraphic controls governing the hydrocarbons migration and emission. The characterization of the oil seepage rates and of the geological setting offshore Cape Kalumba provides further elements to better understand the generation and migration of oil associated with the hydrothermal systems in the East African Rift lakes.

## 2. Geological setting

Major lacustrine basins formed as consequence of the evolution of the western branch of the East African Rift (EAR). Lake Tanganyika is the largest and deepest of Africa's rift lakes, with a N-S length of 650 km and maximum depth of 1470 m (Coulter, 1991). The present-day lake setting is governed by the interplay of faults belonging to the principal structural trends of the EAR system (Rosendahl et al., 1986; Sander and Rosendahl, 1989). Since the Miocene, the sedimentary basin occupied by Lake Tanganyika has developed asynchronously as three, eventually-connected, basins: the central, northern and southern basins beginning at ca. 12 Ma, 7-8 Ma and 2 Ma, respectively (Cohen et al., 1997, 1993; Lezzar et al., 1996). These three basins are further divided into seven asymmetric sub-basins that are delineated by half-graben structures, of which the main bounding faults alternate on the east and west margins of Lake Tanganyika (Burgess et al., 1988; Sander and Rosendahl, 1989). Throw on the bounding faults is up to 8 km, and the faults are responsible for the deposition of a more than 4 km-thick sedimentary column in the lake depocenters (Burgess et al., 1988; Rosendahl et al., 1986).

Proterozoic lineaments that have been reactivated during recent rifting control the emplacement of sub-lacustrine hydrothermal seeps that are documented in the NW sector of Lake Tanganyika, at Pemba (Bujumbura Sub-basin) and Cape Banza (Rumonge Sub-basin) (Pflumio et al., 1994) (Fig. 1). In Pemba, hot water is vaporised in the subsurface and mixed with the lake water in the shallow subsurface. Otherwise, the hydrothermal activity at Cape Banza is characterised by the emission of lake water that has been exposed to high temperatures when in contact with basement rocks and that later migrated through a network of fractures and pipes within the subsurface (J. Tiercelin et al., 1993). Despite the fact that Lake Tanganyika has not experienced volcanism within close proximity, it is likely that the hydrothermal manifestations originated due to shallow intrusions of magmatic bodies, which have been interpreted as the possible initial stage of development of a new volcanic province forming in this area of the EAR (Coussement et al., 1994).

The Cape Kalumba oil seeps occur a few kilometres offshore of the southern end of the Ubwari Peninsula and near the boundary between the Rumonge and Kigoma Sub-basins (Fig. 1). The Ubwari Peninsula is an approximately N-S oriented horst that partially separates the Bujumbura and Rumonge Sub-basins, and is delimited by the East and West Ubwari Faults (Coussement et al., 1994; Simoneit et al., 2000). The East Ubwari Fault (EUF) controlled the formation of the Rumonge Sub-basin, which reaches ~1150 m depth at the Ubwari Peninsula. In this area, the EUF displaces Proterozoic high-grade orthogneiss and metasediments basement against Upper Miocene to Recent sedimentary cover (Coussement et al., 1994; Lezzar et al., 1996; Simoneit et al., 2000). These Proterozoic lineaments were reactivated during recent rifting and are associated with the shallow magmatic intrusions (Coussement et al., 1994) that may have caused local hydrothermal maturation of source rocks (Pflumio et al., 1994).

## 3. Materials and Method

Satellite images of offshore Cape Kalumba, covering the timespan from 2002 to 2006, are from the Global Offshore Seepage Database (GOSD) assembled by CGG | NPA Satellite Mapping. One or more satellite scenes imaged oil slicks during each considered year. "Side-looking" Synthetic Aperture Radar (SAR) images were acquired by four C-band SAR satellites (ERS-2, Envisat, Radarsat-1 and Radarsat-2), integrated by non-routine data collected by X- and L- band satellites (ALOS PALSAR, TerraSAR-X, TanDEM-X, COSMO-SkyMed). We used two additional Google Earth historical images to enhance the time coverage of GOSD data in the years 2008 and 2009 (Fig. 2).

In the subaqueous environment, hydrocarbons commonly migrate vertically through the water column as gas bubbles coated with an oil film or as distinct oil drops (Garcia-Pineda et al., 2010; Johansen et al., 2017; Mazumder and Saha, 2004; NPA, 2013). The continuous emission of oil produces coalescent slicks on the water surface that are transported by currents and winds. The viscoelastic properties of oil films are responsible for dampening the water surficial wavelets making the slicks detectable by satellite sensors (Garcia-Pineda et al., 2010; Mazumder and Saha, 2004; McCandless and Jackson, 2004).

Resolution of SAR images varies depending on the technical specifications of satellite sensors and processors. Image resolution is ca. 20-30 m, although image data are normally re-sampled to a uniform pixel size of 12.5 m (156 $m^2$) by CGG | NPA. At least four pixels are needed to recognise a pattern thus, slicks shorter than ca. 60 m are usually not recorded. Numerous oceanographic features generate effects that can be detected on SAR imagery. Natural features such as shallow water topography, biogenic natural films from plankton/algae and wind shadow effects can all create regions of sea surface slicking. In addition to those features there are additional artificial oil-based pollutants from shipping, industry and hydrocarbons exploration which further act to obfuscate signs of natural oil seepage slicks under SAR. Whilst much effort has been placed into automated methods for natural seepage slick detection (Suresh et al., 2015), these often run afoul of misclassification and false positives within the variety of sources of sea surface slicking and the diverse range of morphologies these can generate on the imagery. At present, manual identification of seepage from SAR imagery acquired over multiple dates is the most reliable method of classifying the sources of slicks observed from SAR. The recognition and interpretation of the slicks on SAR images has been performed by CGG | NPA. A qualitative approach was taken to slick classification based on the observed morphologies of the slicks, with categorisation in three groups according to their origin: oil seepages, oil pollution and non-oil natural films (Fig. 3). Slicks have been ranked S1 to S3 in descending interpretation confidence level, where S1 slicks are usually associated with intense, persistent oil seepage that produces long and narrow slicks with sharp edges (Figs. 4a,b). S2 and S3 slicks are still spatially well-defined but have progressively less distinguishing features. Oil pollution slicks are thicker than natural seepage and occur in two categories, P1 (fresh pollution) and P2 (remnant pollution). Unassigned (UA) and Priority Unassigned (PU) are further slick categories, which have ambiguous characteristics that cannot be conclusively differentiated as pollution or seepage based only on satellite data. PU, where oil surfactant is more probable, keeps some characteristics that are more indicative of possible oil seepage with respect to UA slicks.

The availability of accessible seismic data the NW Lake Tanganyika is limited, and when present, it has relatively large lines spacing. We used the legacy seismic line 256 acquired by the PROBE project of Duke University (Rosendahl, 1988) to reconstruct the local subsurface setting below the Cape Kalumba oil slicks. This line runs along a NW-SE direction for a total length of circa 20 km from Cape Kalumba to the lake center (Fig.1). The reflection seismic line 256 is a 24-fold stacked, unmigrated time section penetrating the first 6 seconds of the subsurface (Scholz and Rosendahl, 1990).

## 4. Results

### *4.1 Oil slicks characteristics*

Satellite images acquired between 2002 and 2009 give time-lapse evidence for the persistence of slicks and variations in their dispersion. The occurrence of 25 individual oil slicks that spread over a lake area of ca. 550 km$^2$ is documented. Single slicks typically form stripes up to 25,6 km long with individual areas up to 15.7 km$^2$ (Tab. 1). The wider slicks are oriented NW-SE and NE-SW, while small linear slicks mostly trend E-W and N-S (Fig. 5). All the slicks are natural oil seepage, but the northernmost linear slicks (PU and UA in Figure 5) cannot be classified based on satellite imagery alone.

Oil slick origin (OSO) (Garcia-Pineda et al., 2010) points are readily recognized in a constrained area ca. 4 km southeast of Cape Kalumba (Fig. 5), which is temporally and spatially consistent in the time lapse series (Fig. 6). The 2005 images show a well-defined alignment of OSOs trending W-E (Figs. 4a,c; 6c). A NW-SE alignment of OSOs is seen on the 2003 and 2008 images (Fig. 6b,e). Unequivocal correlation between slicks and their respective OSOs is straightforward on the SAR images. Small linear slicks are generated by single OSOs that are usually located at their most proximal detectable end. Major slicks typically originate from clusters of closely-spaced OSOs that identify discrete minor slicks, which coalesce progressively moving away from the emission points; eventually they form a single large slick. Most OSOs cluster into a well-defined area SE of Cape Kalumba, suggesting that this is the focus of seepage on the lake floor (Fig. 5).

### *4.2 Subsurface setting*

In the absence of direct observation of the lake floor, to constrain the hydrocarbon fluid subsurface migration paths and to estimate the location of seeps, we used a PROBE Project reflection seismic line, which is oriented NW-SE and transects the area where OSOs occur (Fig. 7). Unfortunately, no borehole data are available in Lake Tanganyika to enable stratigraphic calibration.

The Lake Tanganyika sedimentary infill accumulates above the top of pre-rift basement (Nyasa Event surface, Fig. 7) (Burgess et al., 1988; Rosendahl, 1988). In the Cape Kalumba area, the syn-rift infill can be divided into lower and upper stratigraphic sequences, which are separated by a major unconformity (Kigoma-Makara Sequence Boundary of Rosendahl (1988), KMSB) that marks significant fluctuations in the lake level (Lezzar et al., 2002; Sander and Rosendahl, 1989; Scholz and Rosendahl, 1988).

The Makara Sequence is the lower sedimentary interval and has a general homogeneous thickness in the central to SE sector, and progressively thins moving northwestward in the area adjacent to the East Ubwari Faults system (Fig. 7). The Makara units show abrupt lateral variations in thickness within short distances evidencing the structural control during the sediment deposition. The Kigoma Sequence lies stratigraphically above the Makara Sequence, with the two sedimentary intervals separated by the KMSB. The occurrence of a small depocentre proximal to the East Ubwari Faults system indicates that these structures controlled the local sediment accumulation during the deposition of Kigoma units. Indeed, the two main depocenters of the Kigoma Sub-basin are located south of the Ubwari Peninsula (Sander and Rosendahl, 1989).

Local tectonic setting is responsible for displacing the basement and for the resulting formation of large tilted fault blocks (Fig. 7). Similar rifting-related structures, such as horsts and down-thrown closures against the major basin bounding faults, have been documented in other areas of the Lake Tanganyika basin and represent potential hydrocarbon plays (Roberts et al., 2015). Within the half-graben basin the tectonic structures cutting the Makara and lower units do not propagate into the overlying Kigoma but rather, they stop in correspondence of the KMSB. A single fault branches and propagates into the Kigoma Sequence, terminating close to the lake floor.

Northwest of the Ubwari channel, the stratal geometry indicates the strike-slip nature of the main faults. These faults are responsible for the lateral displacement of the succession, as has been documented in other parts of the basin (Sander and Rosendahl, 1989). Normal faulting is documented both in the area further offshore and in the area near to the East Ubwari Faults system.

## 5 Discussion

### *5.1 Hydrothermal activity and hydrocarbons*

The generation of hydrocarbons by the contact of buried organic matter with hydrothermal waters is a relatively rare, but known phenomenon. The occurrence of *hydrothermal petroleum* has been documented in various locations worldwide, such as the Guaymas Basin (Peter et al., 1991), Middle Valley and Escanaba Trough (NE Pacific Ocean) (Simoneit et al., 1992; Simoneit and Kvenvolden, 1994), Kagoshima Bay (Japan) (Yamanaka et al., 2000), Waiotapu region in New Zealand (Czochanska et al., 1986), Uzon caldera (Kamchatka) (Bazhenova et al., 1998), and Yellowstone National Park (Clifton et al., 1990).

Hydrothermal activity is well-known in northern Lake Tanganyika (Botz and Stoffers, 1993; Tiercelin et al., 1993b; Coussement et al., 1994; Pflumio et al., 1994). Venting of hot water (65-80°C) is associated with the emission of $CO_2$ (60-90 % of total gas) (Botz and Stoffers, 1993; Tiercelin et al., 1993) and hydrocarbon gas ($C_1$ to $C_6$), of which methane is the predominant fraction (68.76-98.87 %) (Botz and Stoffers, 1993). The methane and light hydrocarbon gases are probably generated by both biogenic and thermocatalytic activity, similar to that documented in the hydrothermal emissions in Lake Kivu (Botz and Stoffers, 1993; Simoneit et al., 2000). An active geothermal system is confirmed by the fluid geochemistry, including stable isotope analysis of $CO_2$, that documents the interaction of the lake water with high-temperature magmatic volatiles (Botz and Stoffers, 1993; Pflumio et al., 1994; Tiercelin et al., 1993). Offshore from the Ubwari Peninsula the interaction between hydrothermal water and fine-grained, lacustrine sediment is evidenced by deuterium enrichment (Pflumio et al., 1994).

Total Organic Carbon (TOC) within sediments of Lake Tanganyika can be up to 12 %, with values above 5-6 %TOC and up to 35 kg hydrocarbons/ton of rock generation potential in the eastern offshore of Ubwari Peninsula (Huc et al., 1990). The sources of organic matter occurring within Pleistocene to present-day sediments consist mainly of bacterial (e.g. cyanobacteria) and algal (e.g. diatom) remains (Huc et al., 1990).

The geochemical characterization of tar balls collected along the coast of Ubwari Peninsula and of Cape Kalumba oil indicate their generation from shallow-buried immature bacterial and algal kerogen deposited during the past 25 kyr (J. Tiercelin et al., 1993). Consequently, the hydrocarbon generation is constrained to a short maturation period that is strongly dependent on the invasion of the shallow sedimentary section by hot hydrothermal fluids. The brief exposure of immature organic matter to the elevated temperatures produced by the hydrothermal system is thus responsible for the generation of the oil (Simoneit et al., 2000; Tiercelin et al., 1993; Tiercelin et al., 1992). A time span of a few tens of thousands of years is thus identified for single-step petroleum generation caused by hydrothermal activity (Kvenvolden and Simoneit, 1990; Simoneit and Kvenvolden, 1994). This differs significantly from that required for conventional thermal maturation of organic matter and petroleum migration during burial, which is orders of magnitude slower.

A pervasive network of migration pathways for hydrothermal water from basement units to the lake floor is necessary. Although geometry and spatial characteristics of the migration pathways are still poorly defined due to lack of suitable data, the fault systems imaged in the seismic lines, together with unresolved sub-seismic fractures, are likely inducing infiltration of hydrothermal fluids into the sedimentary succession.

Seeping oil is assumed not to have been significantly biodegraded (Simoneit et al., 2000), which is indicative of its rapid rise from subsurface temperatures above 60 °C, below which accelerated biodegradation occurs. It is implicit that the areal extent of organic matter affected by hydrothermal maturation is large enough to sustain the seeps activity for more than a century.

*5.2 Controls on seepage and oil slicks characteristics*

Persistence of oil slicks through time is indicative of oil seepage (De Beukelaer et al., 2003; Jatiault et al., 2017; Körber et al., 2014; Orange et al., 2009) and the satellite data from Cape Kalumba in the period 2002 to 2009 prove this to be the case (Fig. 6). This is hardly surprising given early geological records of oil and tar at this location (Nicolas, 1898) and more recent analyses of tar balls (Simoneit et al., 2000; Tiercelin et al., 1993). Persistence of oil slicks and OSOs are compelling evidence that the slicks relate to an active macro-seepage system and not to occasional emission events.

The East Ubwari Faults system coincides with a marked shallowing at the lacustrine margin where faults are mapped close to the lake-floor and sedimentary units thin and steepen shoreward (Fig. 7). Evidence of the alignment of some OSOs at Cape Kalumba (2005, 2003 and 2008, Fig. 4) is likely to be associated with the spatial distribution of lake-floor seeps, specifically relating fractures or faults with the OSOs distribution. We interpret the fault zone as the main control on seeps location. Seeps are probably associated with multiple fractures from which oil is leaking simultaneously. This is supported by the observation of compositional differences in the seeps, which indicates the contribution of various seeps over an extensive area of the lake floor (Simoneit et al., 2000). Similar fracture-seep relationships are characteristic of seepage sites worldwide (Miller and Nur, 2000; Plaza-Faverola et al., 2014). The fault system is also interpreted to control the origin of the PU and UA oil slicks documented to the north of the main seepage area, due to similarities in the subsurface setting and position of OSOs through time. Because not all OSOs are aligned and documented throughout the time span investigated they reflect a transient situation in the activity of individual seeps. It is implicit that dilation of the tectonic discontinuities that sustain seepage varies through time, which in turn relates to variations of pore-fluid pressure in the system and to the location and rate of flow from seeps (Miller and Nur, 2000; Plaza-Faverola et al., 2014).

The geometry of sedimentary units suggest that the oil could migrate up-dip and laterally along the strata towards the basin margin, until it escapes from the strata termination on the border faults. This process may support the prolonged focused activity of the oil seeps, providing a continuous supply of oil from the surrounding areas. In fact, coring and high resolution seismic surveys in similar areas of the lake evidenced that the uppermost 100m of sediments have been deposited since the Late Pleistocene (Tiercelin et al., 1994, 1992), thus limiting the interval of the 25 kyr old source rock at Cape Kalumba to *ca* the upper 20m of sediment (if a constant sedimentation rate is assumed).

Although lake circulation adjacent to the Ubwari Peninsula may cause some offset between seepage and OSOs we assume that they approximately overlie lake-floor seeps due to the consistency of their location through time despite lake-current variability and seeps location above the major faults. In general, the spread of oil slicks on water surfaces is driven by shallow wind-driven currents. In Lake Tanganyika this type of current is sustained by persistent southeasterly trade winds throughout the dry season (June to August), which decrease in intensity during the rainy season (Docquier et al., 2016; Podsetchine and Huttula, 2000; Verburg and Hecky, 2003). Along the coast, these trade winds combine with diurnal E-W breezes and upslope-downslope winds (Podsetchine and Huttula, 2000). The wind regime in the northern sector of Lake Tanganyika controls the direction of surficial currents down to 50 m lake depth, with daily variations in wind direction (Podsetchine and Huttula, 2000). Consequently, the dispersion of oil slicks on the lake surface corresponds to the interaction of two principal wind orientations, SE-NW and E-W. Some slicks are however dispersed southward (Fig. 5), which indicates the occasional influence of localized currents probably generated by the coastal geomorphology. The occurrence of longshore currents is likely to be responsible for slicks that strand tar balls on the shores of the Ubwari Peninsula (Simoneit et al., 2000).

*5.3 Seepage rates*

Attempts to estimate the exact discharge rates from underwater seeps are still rudimentary and are complicated by the temporal variability of seepage. An estimation of the oil emission rate and volumes is obtained analysing the geometrical proprieties of slicks. The average slick thickness is ca. 0.1 µm (Macdonald et al., 1993; MacDonald et al., 2015). Adopting a conservative approach to estimate the amount of oil discharged by the seeps in Lake Tanganyika, we assume that the slicks are uniformly distributed and have the average thickness of 0.1 µm. Unfortunately, the exact thickness of the singleindividual slicks cannot be determined from our SAR images.

The velocity of slick propagation is influenced by both wind and water current velocities, while the oil composition does not appear to have a significant role. Water current velocity attributable to wind is equal to ca. 3-4% the velocity of wind (Espedal and Twahl, 1999), which in northern Lake Tanganyika averages 2-4 m $s^{-1}$ between the dry and wet seasons (Docquier et al., 2016). There are no data records of water current velocity in the lake. Assuming the wind is the only factor controlling the water movement, the estimated slick propagation velocity in this sector of the lake is a minimum of 0.09 m $s^{-1}$ for a 3 m $s^{-1}$ wind. Given the general velocity of slick propagation and slick length, estimates of the time needed for their formation are made. Thus, slicks at Cape Kalumba have a formation time that ranges between 2 and 79 hours, with most of the slick formation times below 30 hours (Table 1).

By considering the thickness of the oil film and the areal extent of slicks, the amount of oil forming individual slicks is determined and ranges between 8.9 and 1900 litres (Table 1). Relating the formation time to the volume of oil, minimum emission rates are derived ranging between 31.28 – 449.39 $m^3$ $y^{-1}$. Despite being an approximate and conservative estimate, the average annual total seepage rate in the Cape Kalumba seeps is ca. 138.7 $m^3$ (2002 to 2009 interval), corresponding to ca. 0.58 $m^3$ $d^{-1}$. This value is consistent with the estimated <1 $m^3$ $d^{-1}$ oil seepage rate from individual seeps in the Gulf of Mexico, a major seepage province (MacDonald et al., 2015), and slightly above the average in the South Caspian Basin (Zatyagalova et al., 2007).

Average annual discharge rates are calculated by considering all the documented slicks (Table 2). During the period 2003 to 2005 the rate of oil emission reduced by more than 50% with respect to 2002. In 2006 the amount of oil discharged increased again, reaching a peak in 2008, then lower again in 2009. These observations demonstrate the cyclic activity of seepage, with alternating periods of more intense seepage and quiescent periods, although more extensive and detailed data are necessary to confirm this. If confirmed, this seepage behaviour could represent alternating discharge and recharge cycles of the fluids accumulation in the subsurface, and fluctuations of the pressure regime, which in turn could regulate dilation and closing of the tectonic discontinuities that feed the seepage system. Similar behaviour has been widely documented in other seeps worldwide (Miller and Nur, 2000; Plaza-Faverola et al., 2014).

## 6 Conclusions

The analysis of subsurface data and of multi-temporal SAR satellite images of the oil slicks offshore Cape Kalumba offers evidence of the geological setting regulating spontaneous oil seepage in Lake Tanganyika, and allows to estimate the oil seepage rate. Seepage activity is governed by the interplay of fractures along the East Ubwari Faults system, the flow of hot water within the hydrothermal circulation system and the generation of hydrocarbons in the shallowest tens of metres of sediment.

Notwithstanding the long-lasting activity and limited areal extent of Lake Tanganyika, the emission rates of the Cape Kalumba seeps are consistent with those of other individual oil seeps in globally-significant provinces. The origin of the Cape Kalumba oil seeps points to a local petroleum system without accumulation capability. However, the Cape Kalumba seeps are an important feature in the framework of Lake Tanganyika and the other East African Rift lakes. Its occurrence indicates that rapid generation of unconventional hydrothermally derived petroleum may occur, and that this oil

may accumulate in the source rock intervals and/or in traps without leaking, if the appropriate conditions are met. Because of the lack of extensive surveys of the deeper areas of Lake Tanganyika we cannot exclude the occurrence of similar sub-lacustrine hydrothermal systems elsewhere in the lake. In the context of petroleum exploration the Cape Kulumba seeps prove the presence of a high grade oil source rock and an active petroleum system. The downside is that if similar systems fed hydrocarbon traps the high temperature would cause rapid thermal degradation if close to the heat source.

Rift lakes of the EAR's western branch are predicted to have mature source rocks in the oil generation window. Consideration of the characterisation of mature oil source rocks should include the influence of possible hydrothermalism. For example, a persistent oil seep recognized in Lake Malawi, located south of Lake Tanganyika, may be either associated with a conventional petroleum system or to a nearby hydrothermal system. Investigation of the influence of the hydrothermal systems is fundamental to evaluation of hydrocarbon charge in future hydrocarbon exploration activity in settings similar to Lake Tanganyika.

**Acknowledgements**

We thank Michael King and CGG | NPA Satellite Mapping for providing us with the GOSD dataset of Tanzania and the permission to publish the SAR images of Cape Kalumba oil seeps.

**Funding**

This research did not receive any specific grant from funding agencies in the public, commercial, or not-for-profit sectors.

**References**

Aminzadeh, F., Berge, T.B., Connolly, D.L. (Eds.), 2013. Hydrocarbon Seepage: From Source to Surface. Published jointly by SEG and AAPG.

Bazhenova, O.K., Arefiev, O.A., Frolov, E.B., 1998. Oil of the volcano Uzon caldera, Kamchatka. Org. Geochem. 29, 421–428. https://doi.org/10.1016/S0146-6380(98)00129-6

Botz, R.W., Stoffers, P., 1993. Light hydrocarbon gases in Lake Tanganyika hydrothermal fluids (East-Central Africa). Chem. Geol. 104, 217–224. https://doi.org/10.1016/0009-2541(93)90152-9

Burgess, C.A.F., Rosendahl, B.R., Sander, S., Burgess, C.A.F., Lambiase, J., Derksen, S., Meader, N., 1988. The structural and stratigraphic evolution of Lake Tanganyika: A case study of continental rifting., in: Manspeizer, W. (Ed.), Triassic-Jurassic Rifting and the Opening of the Atlantic Ocean. Elsevier, Amsterdam.

Capart, A., 1949. Sondages et carte bathymétrique du Lac Tanganika. Explor. Hydrogeol. du Lac Tanganika.

Clifton, G., Midway, D.C., Tx, U.S.A., Simoneitt, B.R.T., 1990. Hydrothermal petroleums from Yellowstone National Park , 5, 169–191.

Cohen, A.S., Lezzar, K.E., Tiercelin A, J.J., Soreghan, M., 1997. New palaeogeographic and lake-level reconstructions of Lake Tanganyika: Implications for tectonic, climatic and biological evolution in a rift lake. Basin Res. 9, 107–132. https://doi.org/10.1046/j.1365-2117.1997.00038.x

Cohen, A.S., Soreghan, M.J., Scholz, C.A., 1993. Estimating the age of formation of lakes: an example from Lake Tanganyika, East African Rift system. Geology 21, 511–514. https://doi.org/10.1130/0091-7613(1993)021<0511:ETAOFO>2.3.CO;2

Coulter, G.W., 1991. Lake Tanganyika and its life. Natural History Museum Publications & Oxford University Press.

Coussement, C., Gente, P., Rolet, J., Tiercelin, J.J., Wafula, M., Buku, S., 1994. The North Tanganyika hydrothermal fields, East African Rift system: Their tectonic control and relationship to volcanism and rift segmentation. Tectonophysics 237, 155–173. https://doi.org/10.1016/0040-1951(94)90252-6

Czochanska, Z., Sheppard, C.M., Weston, R.J., Woolhouse, A.D., Cook, R.A., 1986. Organic geochemistry of sediments in New Zealand. Part I. A biomarker study of the petroleum seepage at the geothermal region of Waiotapu. Geochim. Cosmochim. Acta 50, 507–515. https://doi.org/10.1016/0016-7037(86)90100-6

De Beukelaer, S.M., MacDonald, I.I., Guinnasso, N.L., Murray, J.A., 2003. Distinct side-scan sonar, RADARSAT SAR, and acoustic profiler signatures of gas and oil seeps on the Gulf of Mexico slope. Geo-Marine Lett. 23, 177–186. https://doi.org/10.1007/s00367-003-0139-9

Docquier, D., Thiery, W., Lhermitte, S., van Lipzig, N., 2016. Multi-year wind dynamics around Lake Tanganyika. Clim. Dyn. 47, 3191–3202. https://doi.org/10.1007/s00382-016-3020-z

Espedal, H.A., Twahl, T., 1999. Satellite SAR oil spill detection using wind history information. Int. J. Remote Sens. 20, 49–65. https://doi.org/10.1080/014311699213596

Garcia-Pineda, O., MacDonald, I., Zimmer, B., Shedd, B., Roberts, H., 2010. Remote-sensing evaluation of geophysical anomaly sites in the outer continental slope, northern Gulf of Mexico. Deep. Res. Part II Top. Stud. Oceanogr. 57, 1859–1869. https://doi.org/10.1016/j.dsr2.2010.05.005

Hu, C., Weisberg, R.H., Liu, Y., Zheng, L., Daly, K.L., English, D.C., Zhao, J., Vargo, G.A., 2011. Did the northeastern Gulf of Mexico become greener after the Deepwater Horizon oil spill? Geophys. Res. Lett. 38, 1–5. https://doi.org/10.1029/2011GL047184

Huc, A.Y., Fournier Le, J., Vandenbroucke, M., Bessereau, G., 1990. Nothern Lake Tanganyika - An Example of Organic Sedimentation in an Anoxic Rift Lake. Lacustrine basin Explor. case Stud. Mod. Analog. 50, 169–186.

Jatiault, R., Dhont, D., Loncke, L., Dubucq, D., 2017. Monitoring of natural oil seepage in the Lower Congo Basin using SAR observations. Remote Sens. Environ. 191, 258–272. https://doi.org/10.1016/j.rse.2017.01.031

Johansen, C., Todd, A.C., MacDonald, I.R., 2017. Time series video analysis of bubble release processes at natural hydrocarbon seeps in the Northern Gulf of Mexico. Mar. Pet. Geol. 82, 21–34. https://doi.org/10.1016/j.marpetgeo.2017.01.014

Körber, J.H., Sahling, H., Pape, T., dos Santos Ferreira, C., MacDonald, I., Bohrmann, G., 2014. Natural oil seepage at Kobuleti Ridge, eastern Black Sea. Mar. Pet. Geol. 50, 68–82. https://doi.org/10.1016/j.marpetgeo.2013.11.007

Kvenvolden, K.A., Simoneit, B.R.T., 1990. Hydrothermally derived petroleum: examples from Guaymas Basin, Gulf of California, and Escanaba Trough, northeast Pacific Ocean. Am. Assoc. Pet. Geol. Bull. https://doi.org/-

Lezzar, K.E., Tiercelin, J.-J., De Batist, M., Cohen, A.S., Bandora, T., Van Rensbergen, P., Le Turdu, C., Mifundu, W., Klerckx, J., 1996. New seismic stratigraphy and Late Tertiary history of the North Tanganyika Basin, East African Rift System, deducted from multichannel and high resolution reflection seismic data and piston core evidence. Basin Res. 8, 1–28.

Lezzar, K.E., Tiercelin, J., Turdu, C. Le, Cohen, A.S., Reynolds, D.J., Gall, B. Le, Scholz, C.A., 2002. Control of normal fault interaction on the distribution of major Neogene sedimentary depocenters, Lake Tanganyika, East African rift Kiram. Am. Assoc. Pet. Geol. Bull. 86, 1027–1059.

MacDonald, I.R., Garcia-Pineda, O., Beet, A., Daneshgar Asl, S., Feng, L., Graettinger, G., French-

Mccay, D., Holmes, J., Hu, C., Huffer, F., Leifer, I., Muller-Karger, F., Solow, A., Silva, M., Swayze, G., 2015. Natural and unnatural oil slicks in the Gulf of Mexico. J. Geophys. Res. Ocean. 120, 8364–8380. https://doi.org/10.1002/2015JC011062

Macdonald, I.R., Guinasso, N.L., Ackleson, S.G., Amos, J.F., Duckworth, R., Sassen, R., Brooks, J.M., 1993. Natural oil slicks in the Gulf of Mexico visible from space. J. Geophys. Res. 98, 16351. https://doi.org/10.1029/93JC01289

MacDonald, I.R., Reilly Jr., J.F., Best, S.E., Venkataramaiah, R., Sassen, R., Guinasso Jr., N.L., Amos, J., 1996. Remote sensing inventory of active oil seeps and chemosynthetic communities in the northern Gulf of Mexico. Hydrocarb. Migr. its Near-surface Expr. 66, 27–38.

Mazumder, S., Saha, K.K., 2004. Detection of Oil Seepages in Oceans by Remote Sensing, in: 6th International Conference & Exposition on Petroleum Geophysics "Kolkata 2006." pp. 1172–1178.

McCandless, S.W., Jackson, C.R., 2004. Principles of Synthetic Aperture Radar, in: Jackson, C.R., Apel, J.R. (Eds.), Synthetic Aperture Radar Marine User's Manual. National Oceanic and Atmospheric Administration, pp. 1–23.

Miller, S.A., Nur, A., 2000. Permeability as a toggle switch in fluid-controlled crustal processes. Earth Planet. Sci. Lett. 183, 133–146. https://doi.org/10.1016/S0012-821X(00)00263-6

Nicolas, H., 1898. Origine marine de certaines espèces de Mollusques en cours de transformation du Lac Tanganyika, in: Association Française Pour l'Avancement Des Sciences, Congrès de Paris, Compte-Rendu. Paris, p. 508−525.

NPA, 2013. Offshore Slick Detection Key Features CGG NPA Satellite Mapping & TREICoL. Edenbridge, Kent, UK.

Orange, D.L., Teas, P.A., Decker, J., Baillie, P., Johnstone, T., 2009. Using SeaSeep surveys to identify and sample natural hydrocarbon seeps in offshore frontier basins, in: Indonesian Petroleum Association Thirty-Third Annual Convention & Exhibition. p. 21.

Peter, J.M., Peltonen, P., Scott, S.D., Simoneit, B.R.T., Kawka, O.E., 1991. 14C ages of hydrothermal petroleum and carbonate in Guaymas Basin, Gulf of California: implications for oil generation, expulsion, and migration. Geology 19, 253–256. https://doi.org/10.1130/0091-7613(1991)019<0253:CAOHPA>2.3.CO;2

Pflumio, C., Boulegue, J., Tiercelin, J.-J., 1994. Hydrothrmal activity in the northren Tanganyika rift, east Africa. Chem. Geol. 116, 85–109.

Plaza-Faverola, A., Pecher, I., Crutchley, G., Barnes, P.M., Bünz, S., Golding, T., Klaeschen, D., Papenberg, C., Bialas, J., 2014. Submarine gas seepage in a mixed contractional and shear deformation regime: Cases from the Hikurangi oblique-subduction margin. Geochemistry, Geophys. Geosystems 15, 416–433. https://doi.org/10.1002/2013GC005082

Podsetchine, V., Huttula, T., 2000. Numerical simulation of wind-driven circulation in Lake Tanganyika. Aquat. Ecosyst. Health Manag. 3, 55–64. https://doi.org/10.1080/14634980008656991

Roberts, D., Chowdhury, P.R., Lowe, S.J., Christensen, A.N., Chowdhury, R.P., Lowe, S.J., Christensen, A.N., 2015. Airborne gravity gradiometer surveying of petroleum systems under Lake Tanganyika , Tanzania, in: ASEG-PESA 2015 – Perth, Australia. pp. 1–4. https://doi.org/10.1071/EG15075

Rosendahl, B.R., 1988. Seismic atlas of Lake Tanganyika, East Africa. Project PROBE, Duke University, Durham, N.C.

Rosendahl, B.R., Reynolds, D.J., Lorber, P.M., Burgess, C.F., Mcgill, J., Scott, D., Lambiase, J.J., Derksen, S.J., 1986. Structural expressions of rifting: lessons from Lake Tanganyika, Africa, in: Frostick, L.E. (Ed.), Sedimentation in the African Rifts. Geological Society of London Special Publication No. 25, pp. 29–43.

Sander, S., Rosendahl, B.R., 1989. The geometry of rifting in Lake Tanganyika, East Africa. J. African Earth Sci. 8, 323–354. https://doi.org/10.1016/S0899-5362(89)80031-4

Scholz, C.A., Rosendahl, B.R., 1990. Coarse-clastic facies and stratigraphic sequence models from Lakes Malawi and Tanganyika, East Africa. Lacustrine basin Explor. - case Stud. Mod. Analog. 151–168.

Scholz, C. a, Rosendahl, B.R., 1988. Low lake stands in lakes Malawi and Tanganyika, East Africa, delineated with multifold seismic data. Science (80-. ). 240, 1645–1648. https://doi.org/10.1126/science.240.4859.1645

Simoneit, B.R.T., Aboul-Kassim, T.A.T., Tiercelin, J.J., 2000. Hydrothermal petroleum from lacustrine sedimentary organic matter in the East African Rift. Appl. Geochemistry 15, 355–368. https://doi.org/10.1016/S0883-2927(99)00044-X

Simoneit, B.R.T., Goodfellow, W.D., Franklin, J.M., 1992. Hydrothermal petroleum at the seafloor and organic matter alteration in sediments of Middle Valley, Northern Juan de Fuca Ridge. Appl. Geochemistry 7, 257–264. https://doi.org/10.1016/0883-2927(92)90041-Z

Simoneit, B.R.T., Kvenvolden, K.A., 1994. Comparison of 14C ages of hydrothermal petroleums. Org. Geochem. 21, 525–529. https://doi.org/10.1016/0146-6380(94)90103-1

Suresh, G., Melsheimer, C., Körber, J.H., Bohrmann, G., 2015. Automatic Estimation of Oil Seep Locations in Synthetic Aperture Radar Images. IEEE Trans. Geosci. Remote Sens. 53, 4218–4230. https://doi.org/10.1109/TGRS.2015.2393375

Talbot, M.R., 1988. The origins of lacustrine oil source rocks: evidence from the lakes of tropical Africa. Geol. Soc. London, Spec. Publ. 40, 29–43. https://doi.org/10.1144/GSL.SP.1988.040.01.04

Tiercelin, J., Boulegue, J., Simoneit, B.R., 1993. Hydrocarbons, sulphides, and carbonate deposits related to sublacustrine hydrothermal seeps in the North Tanganyika Trough, East African Rift, in: Parnel, J., Kucha, H., Landais, P. (Eds.), Bitumens in Ore Deposits. Springer-Verlag, Berlin, pp. 96–116. https://doi.org/10.1007/978-3-642-85806-2

Tiercelin, J., Cohen, A.S., Soreghan, M.J., Lezzar, K.-E., 1994. Pleistocene-modern deposits of the Lake Tanganyika rift basin, East Africa: A modern analog for lacustrine source rocks and reservoirs, in: Lomando, A.J., Schreiber, B.C., Harris, P.M. (Eds.), Lacustrine Reservoirs and Depositional Systems. SEPM Core Workshop Notes, Vol. 19, pp. 37–59. https://doi.org/10.2110/cor.94.01.0037

Tiercelin, J., Pflumio, C., Boulègue, J., Jussieu, P., Cedex, P., Gente, P., 1993. Hydrothermal vents in Lake Tanganyika , East African Rift system. Geology 21, 499–502.

Tiercelin, J., Soreghan, M., Cohen, A.S., Lezzar, K.E., Bouroullec, J.-L., 1992. Sedimentation in large rift lakes: example from the Middle Pleistocene—Modern deposits of the Tanganyika Trough, East African Rift System. Bull. Centres Rech. Explor. Elf Aquitaine.

Van Dort, G., Burges, P., Burden, P., Cloke, I., Ngapurure, U., Stannard, B., Irene, J., Kisekelo, J., Corrigan, S., Visser, R., Grobbler, N., Steyn, A., Kubheka, N., Cowley, S., Colmain, E.O., Rindfuss, R., Maier, J., 2010. UGANDA EXPLORATION: AN OVERVIEW.

Verburg, P., Hecky, R.E., 2003. Wind Patterns, Evaporation, and Related Physical Variables in Lake Tanganyika, East Africa. J. Great Lakes Res. 29, 48–61. https://doi.org/10.1016/S0380-1330(03)70538-3

Vis, G.-J., 2017. Geology and seepage in the NE Atlantic region. Geol. Soc. London, Spec. Publ. 447, SP447.16. https://doi.org/10.1144/SP447.16

Wang, Y., Chen, D., Song, Z., 2013. Detecting surface oil slick related to gas hydrate/petroleum on the ocean bed of South China Sea by ENVI/ASAR radar data. J. Asian Earth Sci. 65, 21–26. https://doi.org/10.1016/j.jseaes.2012.08.016

Yamanaka, T., Ishibashi, J., Hashimoto, J., 2000. Organic geochemistry of hydrothermal petroleum generated in the submarine Wakamiko caldera, southern Kyushu, Japan. Org. Geochem. 31, 1117–1132. https://doi.org/10.1016/S0146-6380(00)00119-4

Zatyagalova, V. V, Andrei, I.Y., Golubov, B.N., 2007. Application of Envisat SAR imagery for mapping and estimation of natural oil seeps in the South Caspian Sea, in: Proc. "Envisat Symposium 2007", Montreux, Switzerland 23–27 April 2007.

**Figure captions**

**Fig. 1** Location and structural setting of northern Lake Tanganyika and Ubwari Peninsula. Inset shows the Lake Tanganyika in the frame of the East African Rift lakes. The hydrothermal field of Cape Banza (CB) and Pemba (PB) are shown. WUF and EUF are West and East Ubwari Faults, respectively. Red line indicates the PROBE seismic line 256 of Figure 7. (Structural setting modified from Coussement et al., 1994; Lezzar et al., 2002; Sander and Rosendahl, 1989). (Bathymetry from Capart, 1949).

**Fig. 2** Map of coverage density of SAR scenes from 2002 to 2006.

**Fig. 3** Scheme of slick categorisation. (Modified from NPA, 2013)

**Fig. 4** Example of SAR images depicting oil slicks offshore Cape Kalumba (see map for location). (**a**) and (**c**) represent S1 slicks occurring in two different moments during 2005. (**b**) is a S2 slick imaged in 2003. White stars mark the oil slick origin for each individual slick. Note how the oil emission points align along a E-W (**a**, **c**) and NW-SE (**b**) directions.

**Fig. 5** Location of the analysed oil slicks with respect to the southern Ubwari Peninsula. The slicks offshore Cape Kalumba are categorised S1 to S3, thus identifying their certain origin from oil seepage. North of the main cluster, 5 further slicks are Priority Unassigned and Unassigned due to their ambiguous characteristics on SAR images. OSO: Oil Slick Origin.

**Fig. 6** Temporal variability of the oil slicks occurrence imaged in the 2002 to 2009 interval. (**e**) and (**f**) are photographs downloaded from Google Earth. It was not possible to recover equivalent SAR images. Oil slick origins are marked with black and white stars.

**Fig. 7** Subsurface geological setting offshore Cape Kalumba. The oil seeps are located above the East Ubwari Faults system that is responsible for the upward migration of hydrothermal water (blue arrows) and the release of the oil in the water column. Oil is generated in the first tens of metres below the lake floor and is likely migrating up-dip (black arrows) towards the basin border faults from the surrounding areas of the basin. KMSB: Kigoma-Makara Sequence Boundary. (Modified from Rosendahl, 1988).

**Tables on separate files**

**Figure 1**



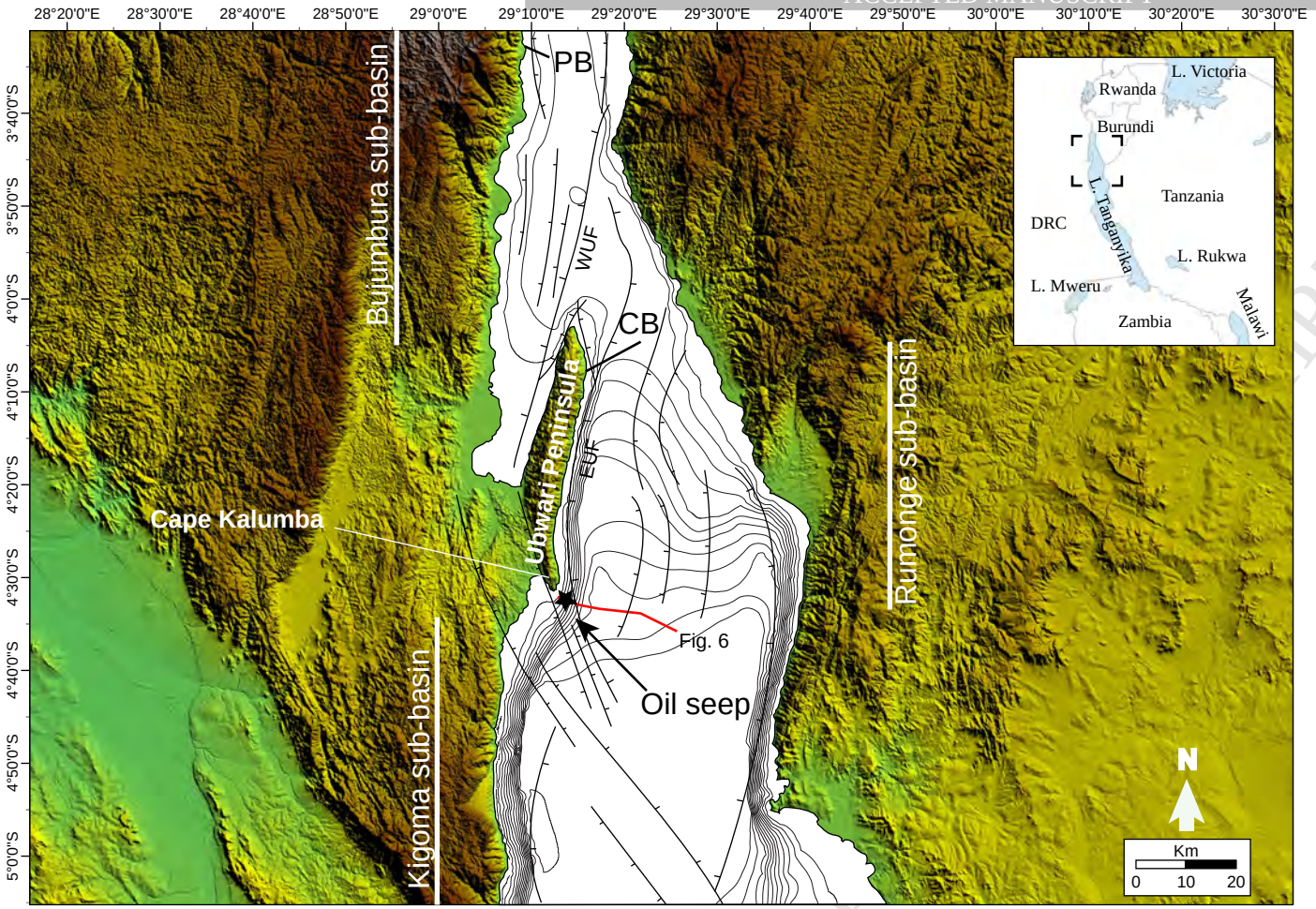

**Figure 2**



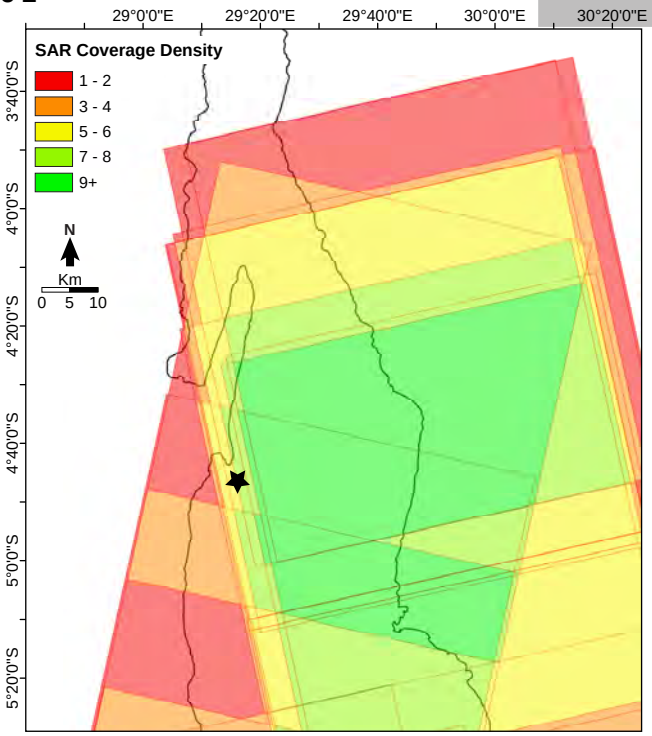

# Figure 3

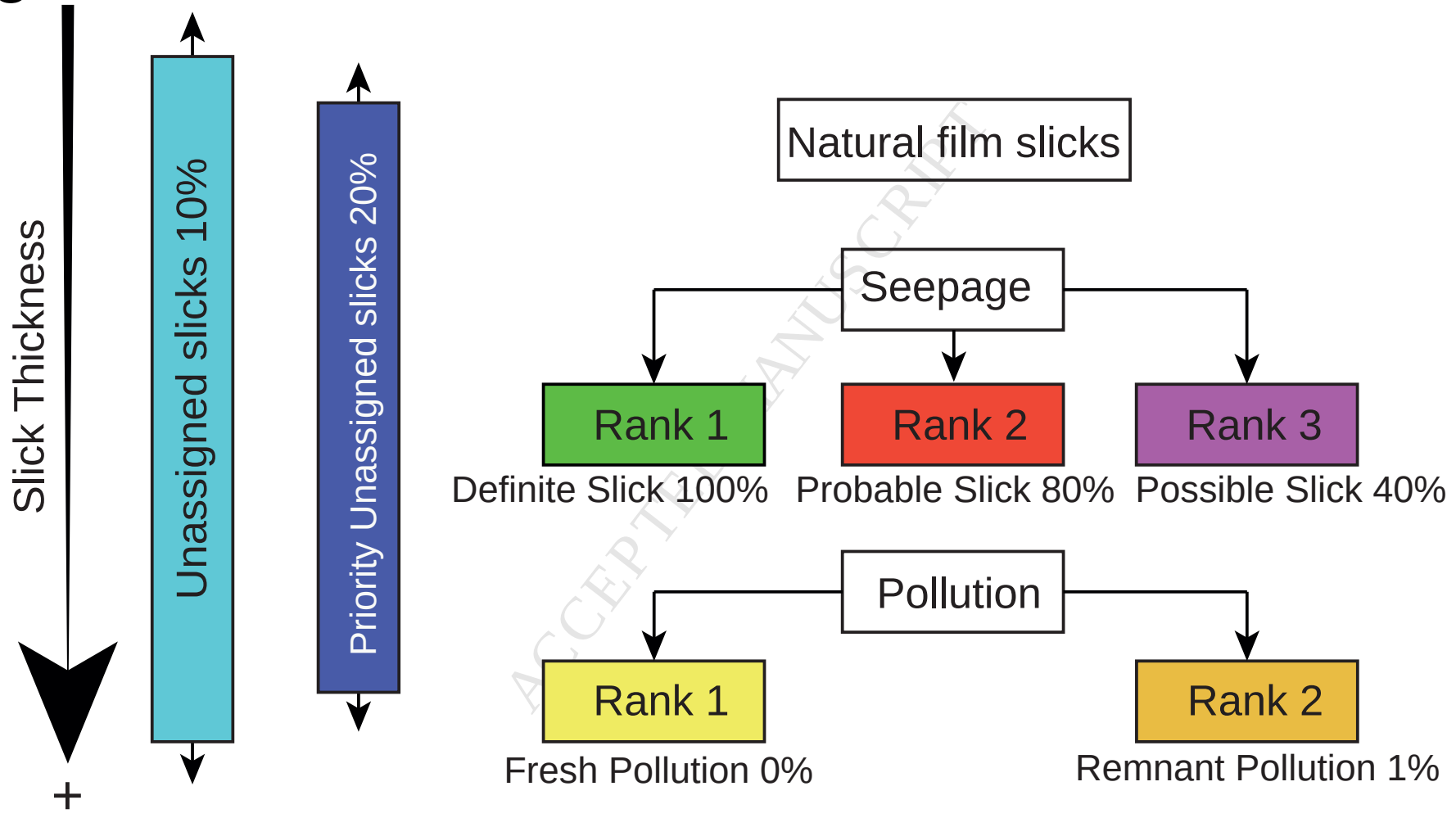

**Figure 4**

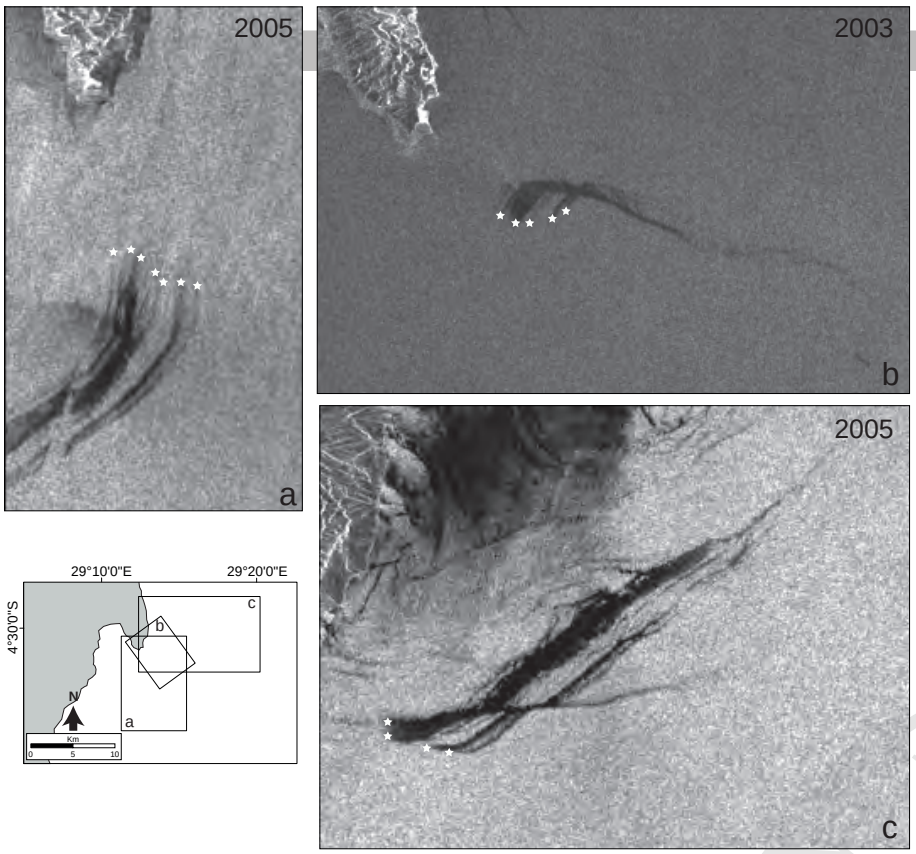

**Figure 5**



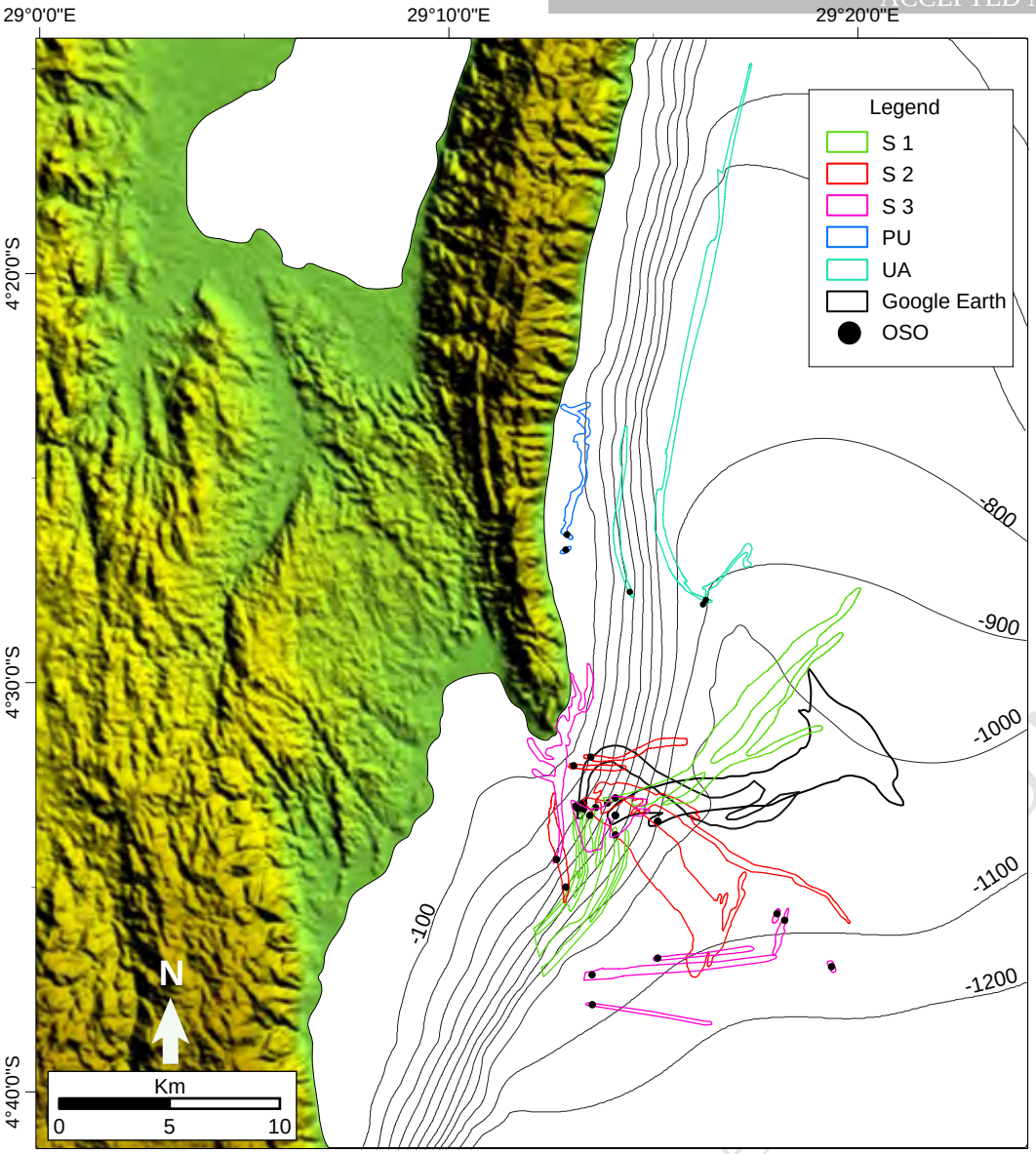

**Figure 6**



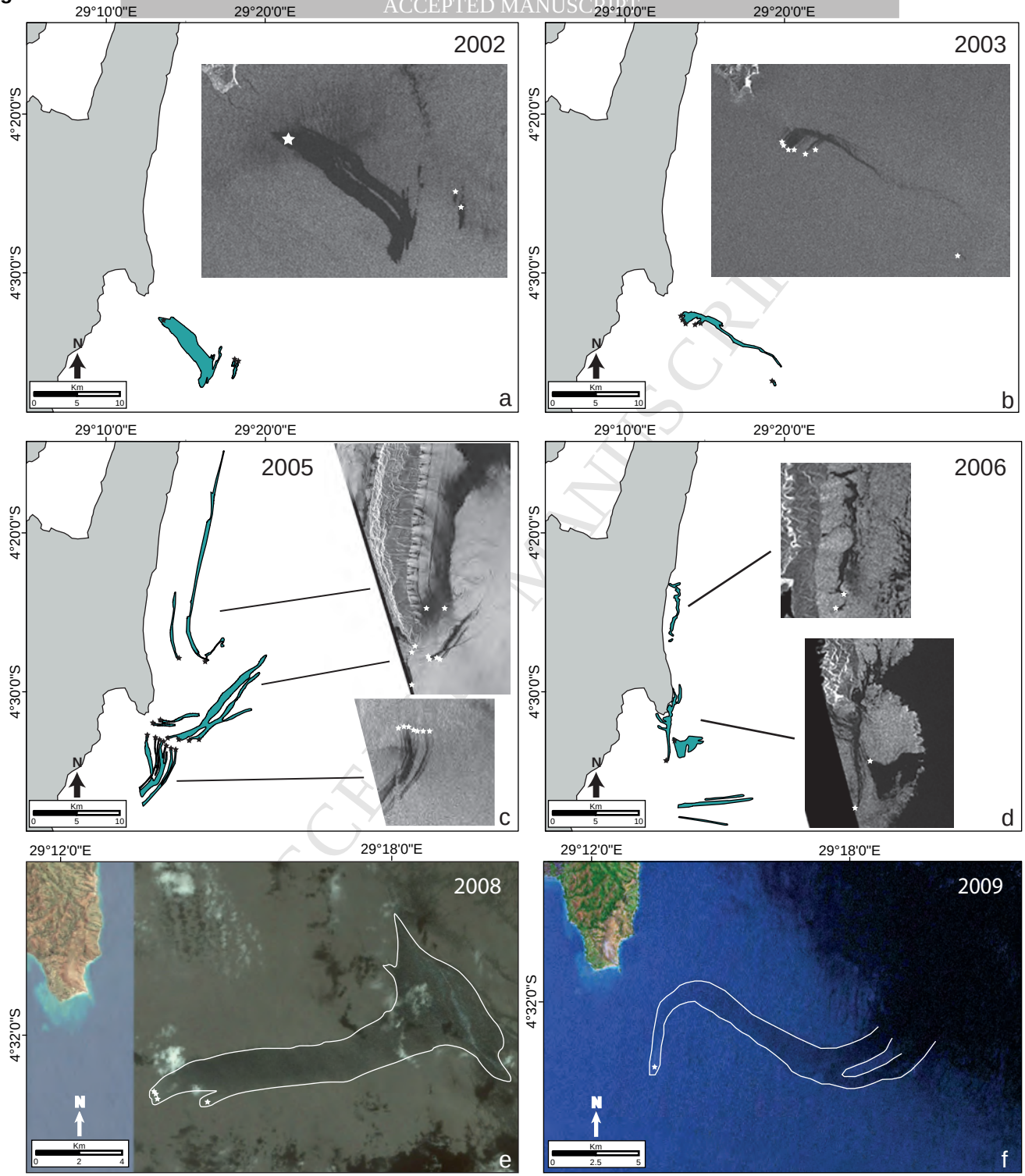

**Figure 7**



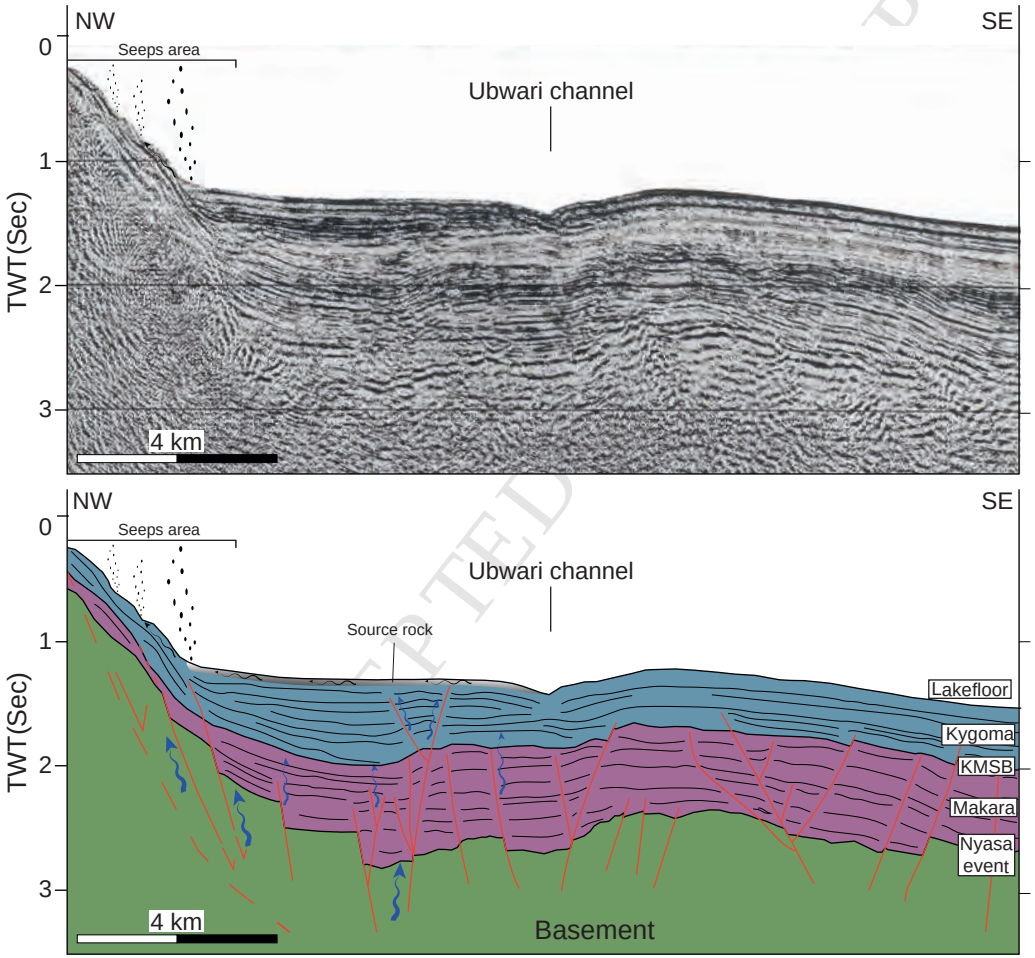

**Table 1.** *Cape Kalumba oil slick characteristics*

| Slick ID | Year | GOSD Category | Long E* | Lat S* | Area ($km^2$) | Length (km) | Volume (l) | Slick formation (hrs) | Rate of emission ($m^3y^{-1}$) |
|---|---|---|---|---|---|---|---|---|---|
| 10966-0005 | 2002 | S2 | 29.2266 | 4.5509 | 15.69 | 9.04 | 1568.90 | 28 | 492.58 |
| 10966-0006 | 2002 | S3 | 29.3005 | 4.5942 | 0.13 | 0.70 | 13.00 | 2 | 52.71 |
| 10966-0007 | 2002 | S3 | 29.3036 | 4.5968 | 0.46 | 2.18 | 46.40 | 7 | 60.41 |
| 10968-0023 | 2003 | S2 | 29.2315 | 4.5491 | 5.89 | 13.23 | 588.70 | 41 | 126.29 |
| 10968-0001 | 2003 | S3 | 29.3227 | 4.6157 | 0.12 | 0.55 | 12.00 | 2 | 61.93 |
| 11006-0013 | 2005 | S1 | 29.2347 | 4.5621 | 2.42 | 7.47 | 242.00 | 23 | 91.95 |
| 11006-0014 | 2005 | S1 | 29.2242 | 4.5541 | 4.02 | 6.95 | 401.50 | 21 | 163.96 |
| 11006-0015 | 2005 | S1 | 29.2184 | 4.5504 | 0.78 | 6.51 | 78.40 | 20 | 34.18 |
| 11006-0016 | 2005 | S1 | 29.2218 | 4.5516 | 0.44 | 4.01 | 44.20 | 12 | 31.28 |
| 12086-0002 | 2005 | S1 | 29.2346 | 4.5470 | 14.32 | 15.57 | 1432.20 | 48 | 261.07 |
| 12086-0001 | 2005 | S2 | 29.2144 | 4.5833 | 1.68 | 4.92 | 167.90 | 15 | 96.86 |
| 12086-0003 | 2005 | S2 | 29.2247 | 4.5304 | 1.22 | 4.92 | 121.60 | 15 | 70.15 |
| 12086-0004 | 2005 | S2 | 29.2177 | 4.5339 | 0.54 | 2.50 | 54.40 | 8 | 61.76 |
| 11006-0017 | 2005 | UA | 29.2703 | 4.4681 | 0.66 | 4.48 | 66.20 | 14 | 41.94 |
| 12086-0009 | 2005 | UA | 29.2715 | 4.4664 | 7.06 | 25.60 | 706.10 | 79 | 78.28 |
| 12086-001 | 2005 | UA | 29.2405 | 4.4630 | 1.67 | 7.80 | 166.90 | 24 | 60.73 |
| 11056-0009 | 2006 | S3 | 29.2519 | 4.6122 | 0.80 | 4.50 | 80.40 | 14 | 50.71 |
| 11056-001 | 2006 | S3 | 29.2252 | 4.6191 | 3.02 | 8.78 | 301.90 | 27 | 97.59 |
| 11056-0011 | 2006 | S3 | 29.2253 | 4.6312 | 0.87 | 5.73 | 87.40 | 18 | 43.29 |
| 11056-0012 | 2006 | S3 | 29.2194 | 4.5514 | 4.48 | 2.90 | 448.40 | 9 | 438.85 |
| 11056-0013 | 2006 | S3 | 29.2107 | 4.5721 | 4.25 | 8.90 | 425.00 | 27 | 135.53 |
| 11056-0014 | 2006 | PU | 29.2144 | 4.4459 | 0.09 | 0.55 | 8.90 | 2 | 45.93 |
| 11056-0015 | 2006 | PU | 29.2150 | 4.4398 | 2.18 | 5.90 | 217.80 | 18 | 104.77 |
| Google Earth 1 | 2008 | NA | 29.2325 | 4.5508 | 19.00 | 12.00 | 1900.00 | 37 | 449.39 |
| Google Earth 2 | 2009 | NA | 29.2206 | 4.5495 | 12.00 | 10.83 | 1200.00 | 33 | 314.49 |

* Geographical coordinates are in WGS 84

**Table 2.** *Average annual oil seepage from Cape Kalumba*

| Year | Total Area ($km^2$) | Total volume (l) | Aver. emission rate ($m^3y^{-1}$) |
|---|---|---|---|
| 2002 | 16 | 1628 | 202 |
| 2003 | 6 | 601 | 94 |
| 2005 | 35 | 3481 | 90 |
| 2006 | 16 | 1570 | 131 |
| 2008 | 19 | 1900 | 449 |
| 2009 | 12 | 1200 | 314 |